

Optimal placement of piezoelectric curve beams in structural shape control

Jian Wang*, Guozhong Zhao and Hongwu Zhang

State Key Laboratory for Structure Analysis and Industrial Equipment,
Department of Engineering Mechanics, Dalian University of Technology, Dalian 116024, P.R. China

(Received September 18, 2007, Accepted October 8, 2008)

Abstract. Shape control of flexible structures using piezoelectric materials has attracted much attention due to its wide applications in controllable systems such as space and aeronautical engineering. The major work in the field is to find a best control voltage or an optimal placement of the piezoelectric actuators in order to actuate the structure shape as close as possible to the desired one. The current research focus on the investigation of static shape control of intelligent shells using spatially distributed piezoelectric curve beam actuators. The finite element formulation of the piezoelectric model is briefly described. The piezoelectric curve beam element is then integrated into a collocated host shell element by using nodal displacement constraint equations. The linear least square method (LLSM) is employed to get the optimum voltage distributions in the control system so that the desired structure shape can be well matched. Furthermore, to find the optimal placement of the piezoelectric curve beam actuators, a genetic algorithm (GA) is introduced in the computation model as well as the consideration of the different objective functions. Numerical results are given to demonstrate the validity of the theoretical model and numerical algorithm developed.

Keywords: shape control; piezoelectric curve beam; finite element method; voltage distribution; placement optimization.

1. Introduction

The using of intelligent materials has attracted much attention in many fields such as biology technology, hydraulics, controllable system, space and aeronautical engineering etc. It is especially used widely in some precise instruments, such as communications satellites and the surface of antenna reflectors. A tiny deformation in these structures could result in a critical error. The structural shape can be controlled by piezoelectric actuators perfectly. A main focus in current research is to find a best distribution of control voltages or an optimal placement of the actuators to keep the structural good performance.

Some finite element theories and models about the piezoelectric materials have been developed for structures integrated with piezoelectric transducers. Tiersten (1969) built a linear piezoelectric constitutive equation firstly based on the linear assumption of electric displacement and fields in the mid of twenty century. Gandhi, *et al.* (1996) considered the effect of the hysteresis loop and repolarization in his formulation. Tzou, *et al.* (1990) developed a piezoelectric isotropic plate element with internal degrees of freedom using classical laminated plate theory. Shah, *et al.* (1993) developed a finite element

*Corresponding Author, E-mail: wangjian_126@163.com

formulation to obtain the static response and stress fields due to the application of electric field to the piezoelectric patches and discussed a simple finite element formulation for in-plane stress analysis of plates with piezoelectric layers. Luo and Tong (2004, 2006) presented a finite element analysis about beams and plates. Chee, *et al.* (2000) developed a theoretical formulation for modeling composite smart structures based on high order displacement theory, in which the piezoelectric actuators and sensors are treated as constituent parts of the entire structural system.

For the shape control, Koconis, *et al.* (1994) analyzed the controlled problem of beam, plate, and shell structures and firstly introduced the idea about the shape control by the inputted voltages in 1994. In the following works, Fitzpatrick (1997) built a mathematic model to control the shape of beam by piezoelectric patches. Degryse, *et al.* (2005) dealt with a novel method to control flexible structures by designing non-collocated sensors and actuators satisfying a pseudo-collocation criterion in the low-frequency domain. Sun and Tong (2005) presented an investigation into design optimization of actuator patterns for static shape control of composite plates with piezoelectric actuator patches. An energy optimization and voltage constraints is described by error functions. Chee, *et al.* (2002) developed a perturbation build-up voltage distribution algorithm to find the optimal voltage distribution for a slope-displacement based objective function. Based on the evolutionary structural optimization method (1997), Merkhujee and Joshi (2002) presented a gradientless iterative technique to find the actuators shape by gradually removing the piezoelectric material based on the residual voltage of elements for shape control. The residual voltage is calculated by subtraction of normalized voltages of initial and current designs. The elements, which have negative residual voltage, are then moved. Nguyen, *et al.* (2007) further developed evolutionary structural optimization method, and presented a new evolutionary algorithm to solve various structural shape control problems of smart composite plate structures with active piezoelectric actuators. The linear least square method and the features of evolutionary strategies are employed to find the applied voltages and shapes for the active piezoelectric actuators, respectively, in order to achieve the desired structural shapes by gradually removing the active piezoelectric material part of the element based on the error function sensitivity number.

Optimization placement is always a focus in the control field especially in recently years about shape control problems. Donthireddy, *et al.* (1996) presented studies obtained by changing the actuator size, location and actuator voltages in composite beams. Lim, *et al.* (1992) found the optimal location for sensors and actuators in flexible structures. Onoda, *et al.* (1993) used GA and simulated annealing algorithms for the optimal location of actuators in the shape control of space trusses. Gaudenzi, *et al.* (1998) employed GA to find the actuator distribution for shape control of beam structures. Han, *et al.* (1999) found the efficient locations of piezoelectric sensors and actuators of a smart composite plate using GA. Peng, *et al.* (2005) built a performance criterion for the optimization of piezoelectric patch actuator locations on flexible plate structures based on maximizing the controllability grammian. Carbonari, *et al.* (2007) derived a formulation that allows the simultaneous distribution of non-piezoelectric and piezoelectric material in the design domain to achieve certain specified actuation movements. Andoh, *et al.* (2004) presented a new approach about the shape control problem with a limited number of discrete actuators. Eigenvalue method was used to improve the transient response.

Although lots of works about shape control and optimization placement have been done, the finite element models and methods of piezoelectric structures are far from full. The integrated shell with beam structure is a major part in modern engineering application. But the researches of shape control of the shell structure strengthened by piezoelectric curve beam are rarely reported. Besides, most of the presented works are based on straight beam and flat plate structure. As well known, the curve shell or beam will be more efficient in the response analysis of curve structures.

On these purposes, this paper presented a finite element formulation for the numerical simulation of the shell structures with piezoelectric beam actuators. A 3-node curve beam element is used here because the using of the quadratic beam element could greatly improve the precision of the model and analysis. The host shell and piezoelectric curve beam are combined with constraint equations directly, which could reduce the number of the degrees of freedom and improve the computation efficiency. The shape control model is built and the control voltage distribution can be obtained by using the LLSM. Furthermore, an optimization model of optimal placement of the piezoelectric curve beam actuators is proposed. In this formulation, the location of the piezoelectric actuator is dealt with discrete variable and the voltage of the piezoelectric actuator is considered as continuous variable. A binary and real coding method of GA is used to solve the optimization problem. The numerical examples of shape control and optimal placement are given to demonstrate the effectiveness of the methods.

2. Finite element model

2.1. 3-node curve beam

A 3-node curve beam is showed in Fig. 1. For a general quadratic curve beam with conventional materials, the coordinate and displacement interpolation formulae can be written in global coordinates system as the following (Bathe 1996):

$$\begin{aligned}
 (x, y, z)^T &= \sum_{i=1}^n N_i(x_i, y_i, z_i)^T + \sum_{i=1}^n \frac{\eta}{2} b_i N_i(V_{y'x}^i, V_{y'y}^i, V_{y'z}^i)^T + \sum_{i=1}^n \frac{\zeta}{2} a_i N_i(V_{z'x}^i, V_{z'y}^i, V_{z'z}^i)^T \\
 (u, v, w)^T &= \sum_{i=1}^n N_i(u_i, v_i, w_i)^T + \sum_{i=1}^n \frac{\eta}{2} b_i N_i A_1 + \sum_{i=1}^n \frac{\zeta}{2} a_i N_i A_2
 \end{aligned}
 \tag{2}$$

where,

$(x, y, z)^T$ is global coordinates of any point in the element;

$(x_i, y_i, z_i)^T$ is global coordinates of node i ;

$(x', y', z')^T$ is local coordinates created on beam cross section;

a_i, b_i are height in ζ direction and width in η direction of node i , respectively;

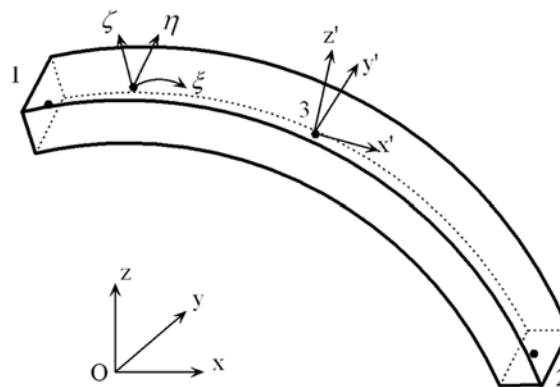


Fig. 1 Sketch of 3-node beam element

$(V_{y'x}^k, V_{y'y}^k, V_{y'z}^k)^T$ is the unit vector in direction η of node i ;

$(V_{z'x}^k, V_{z'y}^k, V_{z'z}^k)^T$ is the unit vector in direction ζ of node i ;

$(u, v, w)^T$ is the displacement components at any point of the element;

N_i is the interpolation function about the 3-node curve beam element, shown as:

$$N_1 = -\frac{1}{2}\xi(1-\xi) \quad N_2 = \frac{1}{2}\xi(1+\xi) \quad N_3 = (1-\xi)(1+\xi) \quad (3)$$

and in Eq. (2),

$$\mathbf{A}_1 = (\theta_{xi} \ \theta_{yi} \ \theta_{zi})^T \times (V_{y'x}^i, V_{y'y}^i, V_{y'z}^i)^T \quad (4)$$

$$\mathbf{A}_2 = (\theta_{xi} \ \theta_{yi} \ \theta_{zi})^T \times (V_{z'x}^i, V_{z'y}^i, V_{z'z}^i)^T \quad (5)$$

where $(\theta_{xi}, \theta_{yi}, \theta_{zi})^T$ is the vector of rotational angles at node i . The vector $(\theta_{xi}, \theta_{yi}, \theta_{zi})^T$ is the listing of the nodal rotations.

The relationship between strain and displacement is:

$$\boldsymbol{\varepsilon} = \mathbf{L}\mathbf{d}_g = \mathbf{L} \begin{bmatrix} \mathbf{J}^{-1} & \mathbf{0} & \mathbf{0} \\ \mathbf{0} & \mathbf{J}^{-1} & \mathbf{0} \\ \mathbf{0} & \mathbf{0} & \mathbf{J}^{-1} \end{bmatrix} \mathbf{d}_m \quad (6)$$

where, \mathbf{J} is Jacobin matrix, and:

$$\mathbf{L} = \begin{bmatrix} 1 & 0 & 0 & 0 & 0 & 0 & 0 & 0 & 0 \\ 0 & 0 & 0 & 0 & 1 & 0 & 0 & 0 & 0 \\ 0 & 0 & 0 & 0 & 0 & 0 & 0 & 0 & 1 \\ 0 & 1 & 0 & 1 & 0 & 0 & 0 & 0 & 0 \\ 0 & 0 & 0 & 0 & 0 & 1 & 0 & 1 & 0 \\ 0 & 0 & 1 & 0 & 0 & 0 & 1 & 0 & 0 \end{bmatrix} \quad (7)$$

$$\mathbf{d}_g = (u_{,x} \ u_{,y} \ u_{,z} \ v_{,x} \ v_{,y} \ v_{,z} \ w_{,x} \ w_{,y} \ w_{,z})^T \quad (8)$$

$$\mathbf{d}_m = (u_{,\xi} \ u_{,\eta} \ u_{,\zeta} \ v_{,\xi} \ v_{,\eta} \ v_{,\zeta} \ w_{,\xi} \ w_{,\eta} \ w_{,\zeta})^T \quad (9)$$

then, using interpolation function, Eq. (9) can be further expressed as:

$$\mathbf{d}_m = [\mathbf{B}_1 \ \mathbf{B}_2 \ \mathbf{B}_3]\mathbf{d} \quad (10)$$

where, \mathbf{d} is the vector including all degrees of freedom of the beam node. So, the relationship between strain and nodal displacement can be written as:

$$\boldsymbol{\varepsilon} = \mathbf{B}\mathbf{d} \quad (11)$$

where, \mathbf{B} is the strain matrix:

$$\mathbf{B} = \mathbf{L} \begin{bmatrix} \mathbf{J}^{-1} & 0 & 0 \\ 0 & \mathbf{J}^{-1} & 0 \\ 0 & 0 & \mathbf{J}^{-1} \end{bmatrix} [\mathbf{B}_1 \ \mathbf{B}_2 \ \mathbf{B}_3] \quad (12)$$

and, \mathbf{B}_i ($i=1, 2, 3$) is:

$$\mathbf{B}_i = \begin{bmatrix} N_{i,\xi} & 0 & 0 & 0 & N_{i,\xi} \left(\frac{\eta}{2} b_i V^i_{y'z} + \frac{\zeta}{2} a_i V^i_{z'z} \right) & -N_{i,\xi} \left(\frac{\eta}{2} b_i V^i_{y'y} + \frac{\zeta}{2} a_i V^i_{z'y} \right) \\ 0 & 0 & 0 & 0 & N_i \frac{1}{2} b_i V^i_{y'z} & -N_i \frac{1}{2} b_i V^i_{y'y} \\ 0 & 0 & 0 & 0 & N_i \frac{1}{2} a_i V^i_{z'z} & -N_i \frac{1}{2} a_i V^i_{z'y} \\ 0 & N_{i,\xi} & 0 & -N_{i,\xi} \left(\frac{\eta}{2} b_i V^i_{y'z} + \frac{\zeta}{2} a_i V^i_{z'z} \right) & 0 & N_{i,\xi} \left(\frac{\eta}{2} b_i V^i_{y'x} + \frac{\zeta}{2} a_i V^i_{z'x} \right) \\ 0 & 0 & 0 & -N_i \frac{1}{2} b_i V^i_{y'z} & 0 & N_i \frac{1}{2} b_i V^i_{y'x} \\ 0 & 0 & 0 & -N_i \frac{1}{2} a_i V^i_{z'z} & 0 & N_i \frac{1}{2} a_i V^i_{z'x} \\ 0 & 0 & N_{i,\xi} & N_{i,\xi} \left(\frac{\eta}{2} b_i V^i_{y'y} + \frac{\zeta}{2} a_i V^i_{z'y} \right) & -N_{i,\xi} \left(\frac{\eta}{2} b_i V^i_{y'x} + \frac{\zeta}{2} a_i V^i_{z'x} \right) & 0 \\ 0 & 0 & 0 & N_i \frac{1}{2} b_i V^i_{y'y} & -N_i \frac{1}{2} b_i V^i_{y'x} & 0 \\ 0 & 0 & 0 & N_i \frac{1}{2} a_i V^i_{z'y} & -N_i \frac{1}{2} a_i V^i_{z'x} & 0 \end{bmatrix} \quad (13)$$

So, the stiffness matrix of 3-node curve beam element can be derived:

$$\mathbf{K}_b = \int_{-1}^1 \int_{-1}^1 \int_{-1}^1 \mathbf{B}^T \mathbf{D} \mathbf{B} |J| d\xi d\eta d\zeta \quad (14)$$

where, \mathbf{D} is the material matrix of beam element.

2.2. Piezoelectric curve beam

If the beam is made from piezoelectric materials and acts as actuators in the structure, the electro-mechanical coupled effects must be considered. The influence from actuators can be regarded as an equivalent force applied on the beam element by the coupling matrix $\mathbf{K}_{u\varphi}$, where, φ represents voltage. The coupling stiffness matrix can be expressed as (Luo and Tong 2004):

$$\mathbf{K}_{u\varphi} = \int_{V^e} \mathbf{B}^T \mathbf{e} \mathbf{B}_\varphi dV \quad (15)$$

where \mathbf{e} is the 6×3 piezoelectric constant matrix in the global coordinates. Employing the stress transformation matrix \mathbf{T}_i (Bathe 1996) and beam element nodal transformation matrix \mathbf{T}_b , It can be

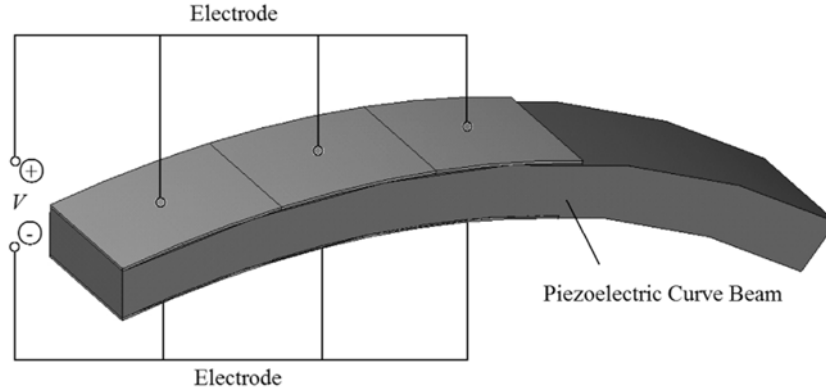


Fig. 2 Electrodes on piezoelectric curve beam

obtained by translating piezoelectric constant matrix e' in local coordinate system:

$$e = T_t e' T_b \quad (16)$$

B_φ in Eq. (15) is the matrix that describes the relationship between electrical displacements and nodal electrical voltage. For a piezoelectric curve beam element, it is assumed the poling direction coincides with the normal direction of its middle surface, as ζ shown in Fig. 1. When the constant voltage is applied to each curve beam element as shown in Fig. 2, B_φ can be obtained by the interpolation function and direction vectors on nodes. It can be given by:

$$B_\varphi = \sum_{i=1}^n \frac{1}{a} N_i (l_{3i}, m_{3i}, n_{3i})^T \quad (17)$$

Substitute Eq. (17) into Eq. (15), the coupled matrix $K_{u\varphi}$ can be obtained.

2.3. Linkage of the beam and shell element

For a flexible shell structure equipped with surface-bonded piezoelectric curve beam actuators, in order to decrease the computing scale and improve the computing efficiency, nodal degrees of freedoms of beam element are merged into shell element. Here, an curve shell element is employed (Cook, *et al.* 2007). Assuming the shell and beam linked directly, the relationship between the shell nodes and beam nodes can be depicted by a set of constraint equations in the local coordinate system, such as shell node 7 and beam node 1, as showed in Fig. 3. Here, there are five degrees of freedom on each shell node and the displacement vector in local coordinate system is $(u'_s, v'_s, w'_s, \theta'_{sx}, \theta'_{sy})^T$. There are six degrees of freedom on each beam node and the displacement vector in local coordinate system is $(u'_b, v'_b, w'_b, \theta'_{bx}, \theta'_{by}, \theta'_{bz})^T$. So:

$$(u'_{b1} \ v'_{b1} \ w'_{b1} \ \theta'_{bx1} \ \theta'_{by1} \ \theta'_{bz1})^T = \mathbf{Q} (u'_{s7} \ v'_{s7} \ w'_{s7} \ \theta'_{sx7} \ \theta'_{sy7} \ \frac{\partial u'_{s7}}{\partial y'})^T \quad (18)$$

where, the sixth degree of freedom of the shell node is expressed as $\partial u'_{s7}/\partial y'$ because it is related to other degrees of freedom of the element (Cook, *et al.* 2007). The matrix \mathbf{Q} in Eq. (18) is the following constraint matrix in local system:

$$\mathbf{Q} = \begin{bmatrix} 1 & 0 & 0 & 0 & \mp \frac{1}{2}(t_s + a) & 0 \\ 0 & 1 & 0 & \mp \frac{1}{2}(t_s + a) & 0 & 0 \\ 0 & 0 & 1 & 0 & 0 & 0 \\ 0 & 0 & 0 & 1 & 0 & 0 \\ 0 & 0 & 0 & 0 & 1 & 0 \\ 0 & 0 & 0 & 0 & 0 & -1 \end{bmatrix} \quad (19)$$

where the sign ' \pm ' represents the location of the beam actuator, over or beneath the host shell. t_s and a are the thickness of the shell element and the height of the beam respectively. Translating the constraint matrix to global coordinate system gets:

$$\mathbf{C} = \mathbf{T}_s^T \mathbf{Q} \mathbf{T} \quad (20)$$

where, \mathbf{T}_s is the translation matrix of the shell element, \mathbf{T} is the translation matrix of the beam element. By the constraint matrix \mathbf{C} , the stiffness of the curve beam can be assembled into the shell element matrix as additional stiffness. The additional stiffness from curve beam can be expressed as:

$$\mathbf{K}_a = \mathbf{C}^T \mathbf{K}_b \mathbf{C} \quad (21)$$

When the actuators is running, the electro-mechanical coupled force on actuators will produce an additional moment on host shell. Alike the additional stiffness of the actuators, the additional moment from actuators can be translated by constraint matrix:

$$\mathbf{P}_a = \mathbf{C}^T \mathbf{K}_{u\varphi} \boldsymbol{\varphi} \quad (22)$$

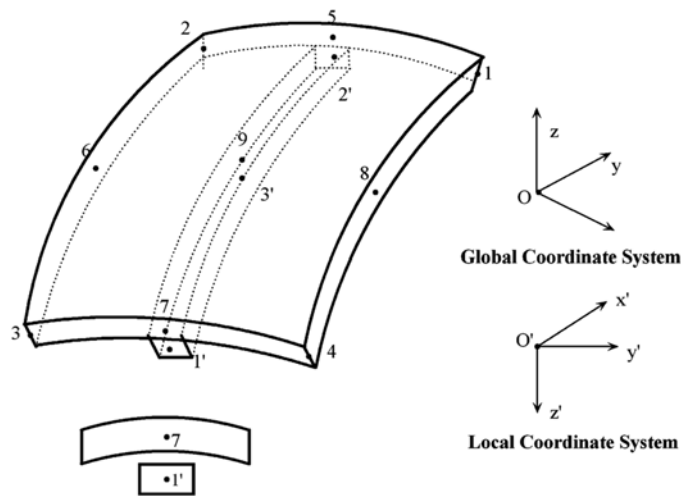


Fig. 3 Sketch of connection between beam element and shell element

2.4. Integrated shell and beam structure

Up to now, the static finite element formulation for the intelligent shell structure equipped with piezoelectric beam actuators can be formed as (Luo and Tong 2004):

$$\mathbf{K}_{uu}\mathbf{u} = \mathbf{K}_{u\varphi}\boldsymbol{\varphi} = \mathbf{P} + \mathbf{P}_a \quad (23)$$

Substitute the Eq. (22) into Eq. (23), it can be written as:

$$\mathbf{K}_{uu}\mathbf{u} = \mathbf{P} + (\mathbf{C}^T - \mathbf{I})\mathbf{K}_{u\varphi}\boldsymbol{\varphi} \quad (24)$$

Where, \mathbf{u} and $\boldsymbol{\varphi}$ are the global displacement and electrical voltage vectors respectively. \mathbf{I} is identity matrix. \mathbf{K}_{uu} is the global stiffness matrix including host shell stiffness and additional stiffness from piezoelectric curve beam:

$$\mathbf{K}_{uu} = \mathbf{K}_s + \mathbf{K}_a \quad (25)$$

\mathbf{K}_s is the host shell stiffness, \mathbf{K}_a is the additional stiffness from piezoelectric beam actuators. From Eq. (24), we can see, voltages can be regarded as external force and it can realize the shape control by adjusting the distribution of the voltages on actuators.

3. Verification of the model

In order to verify the model discussed above, a square of sphere shell surface integrated with piezoelectric beams as shown in Fig. 4 is employed in this section. The radius of the sphere surface is 0.05 m, the central angle of the sphere shell is 23.5 degrees (linear distances between A and B, B and C are all 0.04 m), and the thickness of the shell is 0.001 m. The width and height of the piezoelectric

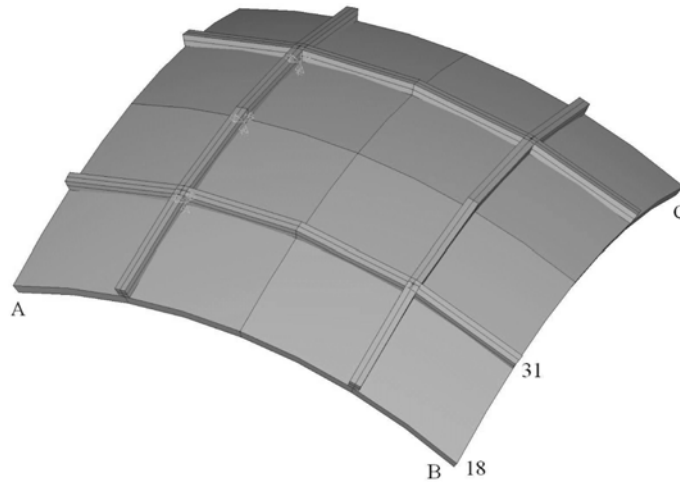


Fig. 4 Model for verification

Table 1 Results of verification

Node No.	Node 18			Node 31		
Deflection	<i>x</i>	<i>y</i>	<i>z</i>	<i>x</i>	<i>y</i>	<i>z</i>
Ansysis	-1.067E-03	-3.490E-03	-8.516E-04	-9.816E-04	-3.223E-03	-5.423E-04
Present	-1.066E-03	-3.470E-03	-8.511E-04	-9.815E-04	-3.221E-03	-5.420E-04
Rotation	<i>Rotx</i>	<i>Roty</i>	<i>Rotz</i>	<i>Rotx</i>	<i>Roty</i>	<i>Rotz</i>
Ansysis	0.912E-01	0.799E-02	-0.125	0.234E-01	-0.388E-01	-0.813
Present	0.903E-01	0.768E-02	-0.119	0.218E-01	-0.378E-01	-0.810

beams are all 0.001 m. The properties of shell and beam elements: Young's Modulus E_e is 20 GPa, Poisson's Ratio ν is 0.3, Piezoelectric Constant e_{31} and e_{32} both are 2 N/(mV). The numerical result will be compared with software ANSYS according to the principle of analogy (Luo and Tong 2004), which supposes the piezoelectric effect is equivalent to the thermal expansion effect by some parameters. BEAM189 and SHELL93 are used in ANSYS model.

Calculating the thermal expansion coefficient according the principle of analogy, the constitute equation of piezoelectric actuator and linear thermal strain can be written as:

$$D\varepsilon - eE = 0 \quad (26)$$

$$\varepsilon = \alpha \cdot \Delta T \quad (27)$$

Where α is the thermal expansion coefficient, If the strain is equivalent, substitute the Eq. (27) into Eq. (26), then:

$$D(\alpha \cdot \Delta T) - eE = 0 \quad (28)$$

Assuming a variation of temperature, 100 degrees, occurs in elements, and the electric field strength E on each actuator is set to 2 V/m. Then the thermal expansion coefficient in Eq. (28) can be calculated as $2.0E-12$. The results of thermal stress analysis by ANSYS and piezoelectric analysis by the model discussed above are listed in Table 1. Due to the symmetric, only two nodes are given.

Table 1 Results of verificationws that the results with the present method matched very well with ANSYS. More importantly, by using of the constraint equations between the piezoelectric curve beams and host shells, the nodes of the piezoelectric curve beam are merged in finite element model. So the computation time can be saved greatly. It is very efficient in the computation of the complicated structures.

4. Optimization model

4.1. Linear Least Square Method (LLSM)

In order to achieve the desired shape which is defined by a set displacement in the reference surface of the host shell, the optimum control voltages must be applied to actuators. The purpose of the shape control is to obtain the voltages by numerical method. The objective function is to minimize the difference between the actuated and desired displacement of the structure. It can be written as the following square error:

$$F(\mathbf{V}) = \sum_{i=1}^n (d_i - d_{oi})^2 \quad (29)$$

where, vector \mathbf{V} is the design variable, which is linear to the nodal displacement. n is the number of the degrees of freedom corresponding to a set displacement. Scalar quantity d_i and d_{oi} represent the actuated displacement and objective displacement of the i th degree of freedom, respectively. For the optimization model, only voltages are considered as external force to actuate the structure shape, substituting the Eq. (24) into Eq. (29) by assuming the external force \mathbf{P} equal to zero, the Eq. (29) can be written as:

$$F(\mathbf{V}) = ((\mathbf{K}_{uu})^{-1}(\mathbf{C}^T - \mathbf{I})\mathbf{K}_{u\phi}\mathbf{V} - \mathbf{d}_o)^T ((\mathbf{K}_{uu})^{-1}(\mathbf{C}^T - \mathbf{I})\mathbf{K}_{u\phi}\mathbf{V} - \mathbf{d}_o) \quad (30)$$

Differentiating the Eq. (30) with respect to voltage variable, we obtain the derivative of the objective function:

$$F'(\mathbf{V})_{\phi} = ((\mathbf{K}_{uu})^{-1}(\mathbf{C}^T - \mathbf{I})\mathbf{K}_{u\phi})^T ((\mathbf{K}_{uu})^{-1}(\mathbf{C}^T - \mathbf{I})\mathbf{K}_{u\phi}\mathbf{V} - \mathbf{d}_o) + ((\mathbf{K}_{uu})^{-1}(\mathbf{C}^T - \mathbf{I})\mathbf{K}_{u\phi}\mathbf{V} - \mathbf{d}_o)^T ((\mathbf{K}_{uu})^{-1}(\mathbf{C}^T - \mathbf{I})\mathbf{K}_{u\phi}) \quad (31)$$

when Eq. (31) is equal to zero, the minimum objective function can be obtained. Assuming $(\mathbf{K}_{uu})^{-1}(\mathbf{C}^T - \mathbf{I})\mathbf{K}_{u\phi} = \mathbf{R}$, the followed formulae can be given:

$$\mathbf{R}^T(\mathbf{R}\mathbf{V} - \mathbf{d}_o) = 0 \quad (32)$$

and,

$$\mathbf{R}^T\mathbf{R}\mathbf{V} = \mathbf{R}^T\mathbf{d}_o \quad (33)$$

solving Eq. (33), the optimum control voltages for the piezoelectric beams can be obtained.

4.2. Placement optimization model by Genetic Algorithm (GA)

Some methods have been studied and applied to the design optimization and shape control. Most of these optimization methods assume that the design variables are continuous, but this is not always valid. In most practical cases, the design variables must be selected in some discrete values instead of continuous. Such as the placement problem of the curve beam actuators discussed in this paper, it can not be solved by continuous model.

In this paper, GA is employed to realize the placement optimization of the actuators. GA is a stochastic search and optimization method (Tang and Gu 2002). It comes from Darwin's principle of survival of the fittest, and it can be applied to commerce, engineering, mathematics, medicine etc. fields. Unlike the gradient-based mathematical optimization methods, GA works with a population and attempt to guide the search toward improvement using the principle of survival of the fittest. Each solution is evaluated by a fitness function (Gu and Tang 2001). It is able to deal with both discrete and continuous design variables by specifying required precision, and it is not limited by restrictive assumptions about the search space, such as continuity and existence of derivatives. So, GA is a powerful design tool in many areas of engineering.

Mixed coding (Tang, *et al.* 2005) scheme of binary and float coding is proposed in this section. Vectors,

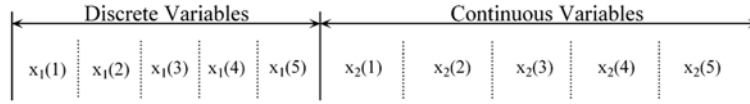


Fig. 5 Mixed coding of the GA

X_1 and X_2 , represent placement information and control voltages respectively.

$$X_1 = X(x_{11} \ x_{12} \ L \ x_{1m})$$

$$X_2 = X(x_{21} \ x_{22} \ L \ x_{2m})$$

x_{1i} ($i = 1,2 \dots m$) is a discrete variable coded by binary, it equals 0 or 1. $x_{1i} = 0$ represents no actuator in this place, $x_{1i} = 1$ represents to keep the actuator in this place. x_{2i} ($i = 1,2 \dots m$) is continuous variable coded by real. The value represents the control voltage of the actuator. The chromosome will be formed according to X_1 and X_2 as shown in Fig. 5.

So, the formulation of the optimization model based on GA can be expressed as:

$$\begin{aligned} & \min F(X_1 \ X_2) \\ & \text{s.t. } G(X_1 \ X_2) \leq C \\ & X_1 = 0 \ \text{or} \ 1 \\ & X_2^L \leq X_2 \leq X_2^U \end{aligned} \tag{34}$$

where, $F(X_1, X_2)$, $G(X_1, X_2)$ are objective function and constraint functions respectively. Eq. (34) will deal with the following two cases. Case 1, in order to minimize the number of actuator, the objective function is the number of actuators and constraint function is the square error from Eq. (30). Case 2, in order to keep the actuated shape as close as possible to the desired shape, the square error is selected as the objective function and the number of actuators is constraint function. The maximum entropy method and surrogate function (Tang, *et al.* 2005) are adopted to deal with the constraints. The penalty method is employed to translate the model to an unconstraint problem. X^L and X^U in Eq. (34) represent lower and upper limits of the design variables.

5. Examples

5.1. Shape control by LLSM

A quarter cylinder shell reflector integrated with piezoelectric curve beam actuators is shown in Fig. 6. The Shell Structure integrated with piezoelectric curve beam. The length of the structure is 50 mm. The radius and thickness of the cylinder shell is 25 mm and 2 mm, respectively. One edge of the structure is clamped and two reversed loads 10N are applied on the opposite edge of the structure. The external force will produce the structural initial deformation shown in Fig. 7 and deformation under external force and piezoelectric curve beam actuators are adopted to control the structural shape. All beam actuators are denoted with the numbers in Fig. 6. The Shell Structure integrated with piezoelectric curve beam. The width and height of the beam section are 1mm. The material properties of shell and

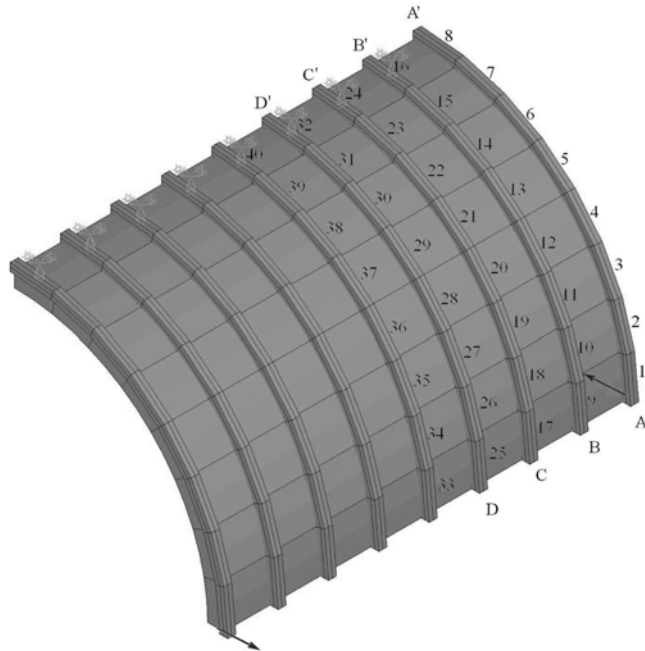


Fig. 6 The Shell Structure integrated with piezoelectric curve beam

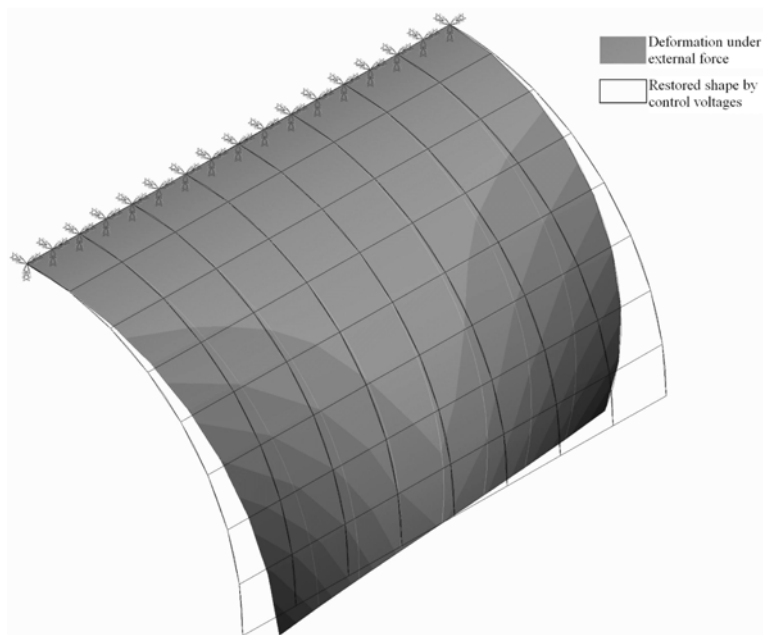


Fig. 7 Comparison between the restored shape and deformation under external force

beam are listed in Table 2.

By applying the control voltage solved by LLSM, the structural shape can be effectively restored. Fig. 7 also gives the restored shape. The square error is $2.1 \times 10^{-6} \text{mm}^2$ (It is $3.7 \times 10^{-2} \text{mm}^2$ if no control

Table 2 Material properties

Materials	Conventional	PZT
Young's Model	76GPa	70GPa
Piezo-Coefficients	0	-5.2 N/(mV)
Poisson's Ratio	0.3	0.25

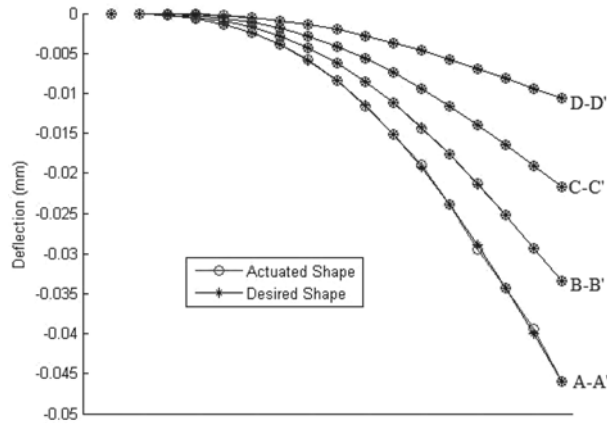


Fig. 8 Comparison between the optimum shape and desired shape on lines AA', BB', CC', DD'

voltage applied). The maximum displacement under external force occurs in the free end of the structure. It is about -0.046 mm. After the shape control, the restored displacement of node is 0.046 mm. Therefore the deformation of node is fully restored. The error ratios of most nodes between the initial displacements and restored displacements are close to zero except few nodes nearby the fixed end. However, the displacements nearby the fixed end are very tiny and they almost have no influence on the structural shape. In order to clearly show the restored displacements and initial displacements, fitting curves along line AA', BB', CC' and DD' are plotted in Fig. 8.

The optimal control voltages are listed in Table 3. Here, due to the symmetric, only the control voltages of the first 40 beam actuators are given. The highest voltage of is 17.22 V and occurs in the actuator 1. From Table 3, we can see that higher voltages occur in the free end of the structure and lower

Table 3 Optimized voltage distribution

EleNo	Vol _{opt}						
1	17.22	11	0.39	21	-0.89	31	-0.12
2	-14.68	12	-0.06	22	-0.11	32	0.00
3	9.17	13	0.70	23	-0.21	33	0.00
4	-5.49	14	0.64	24	0.00	34	0.00
5	2.43	15	0.59	25	0.49	35	0.00
6	-0.24	16	0.00	26	-0.77	36	0.00
7	0.47	17	-0.24	27	0.23	37	0.00
8	0.00	18	-0.47	28	-0.50	38	0.00
9	1.66	19	-1.52	29	-0.15	39	0.00
10	1.19	20	-0.39	30	-0.21	40	0.00

voltages nearby the fixed end. Especially, control voltages of some actuators are zero, which shows not all actuators are necessary. Therefore, accounting for the economy and practicability, the optimal placement of piezoelectric actuators will be an important work.

5.2. Placement optimization by GA

5.2.1. Case 1: Minimizing the number of piezoelectric beam actuators

In this case, the same structure as example 1, the number of the actuators is set as objective function using the model Eq. (34). For the symmetric, Only 40 discrete variables about the actuators' placement information and 40 continuous variables about the voltages on corresponding actuators are set as design variables in the model. The voltages are limited to $[-50V, 50V]$. Square error is used as constraint function to ensure the precision of the shape control. Its upper bound is set to $20.00 \times 10^{-6} \text{mm}^2$.

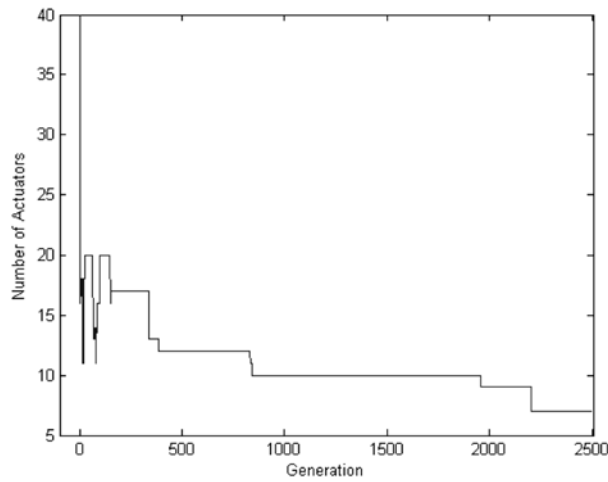


Fig. 9 Iteration history of the objective function (the number of the actuators)

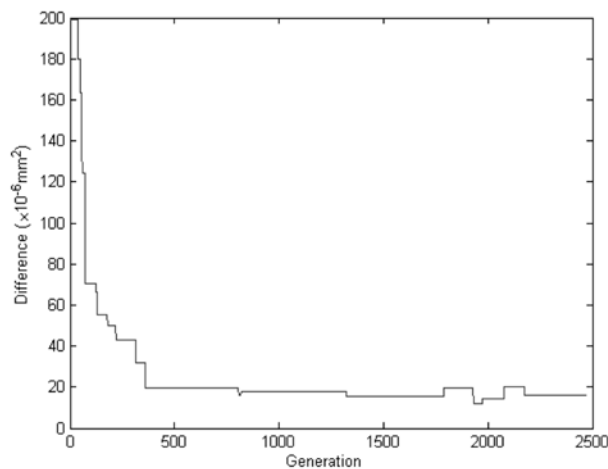


Fig. 10 Iteration history of the constraint function (square error: 10^{-6}mm^2)

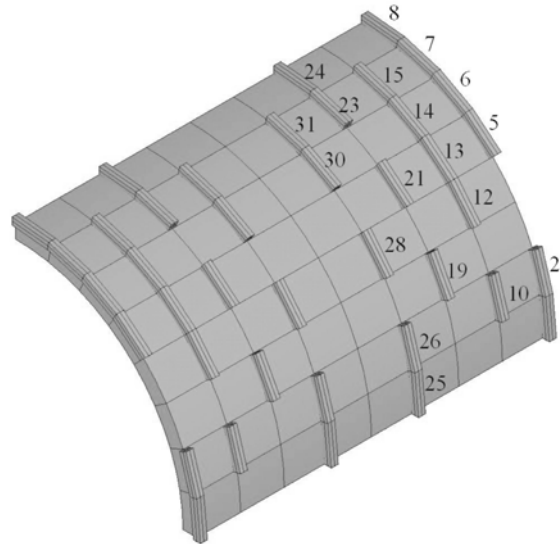


Fig. 11 Placement of the piezoelectric actuators at 36 iteration steps (40 actuators are kept)

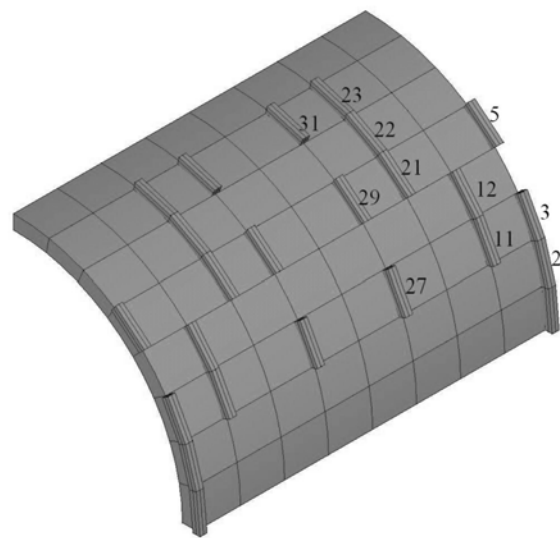


Fig. 12 Placement of the piezoelectric actuators at 398 iteration steps (24 actuators are kept)

After 2500 iteration steps, an optimal result can be obtained. The number of the actuators declines to 7 sharply. It means that only 14 piezoelectric actuators are kept in the optimal placement model. The square error in optimized model is $15 \times 10^{-6} \text{mm}^2$, which satisfies the required precision. Comparing to the maximum desired displacement 0.046 mm, the maximum optimized displacement actuated by the reversed control voltages is 0.047 mm, the error ratio is only 2.1%. Iteration history of the objective function and constraint function are plotted in Fig. 9 and Fig. 10, respectively. Here, there is an oscillation at the initial stage of the iteration as shown in Fig. 9, this is for some complicated problems, GA can not find a feasible individual at the beginning of the iteration. But some individuals which are potential and near to the feasible field are selected. This is useful to find the feasible and optimum

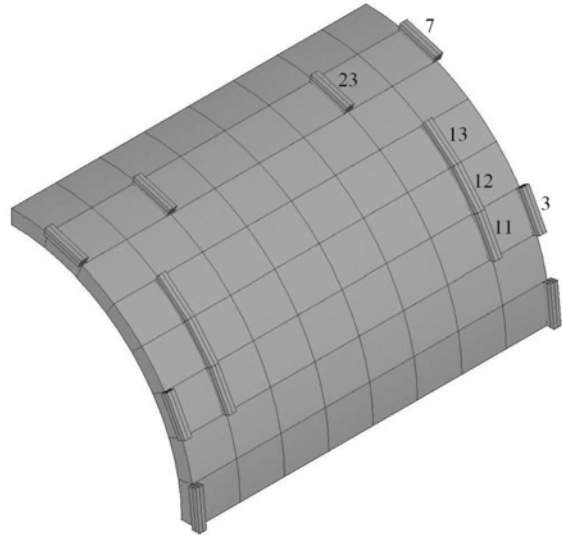


Fig. 13 Optimal placement of piezoelectric actuators (14 actuators are kept at last)

Table 4 Voltages on distributed actuators

No.	1	3	7	11	12	13	23
Voltages	13.6	-6.5	-14.9	-4.1	-21.1	26.7	-39.2

individuals. In order to show the change of placements of the actuators in the iteration process, the placements of the actuators at different iteration steps are given in Figs. 11~13. The optimal control voltages of actuators are listed in Table 4.

5.2.2. Case 2: Minimizing the square error

If only 24 actuators are available, the object is to actuate the shape of the structure as close as possible

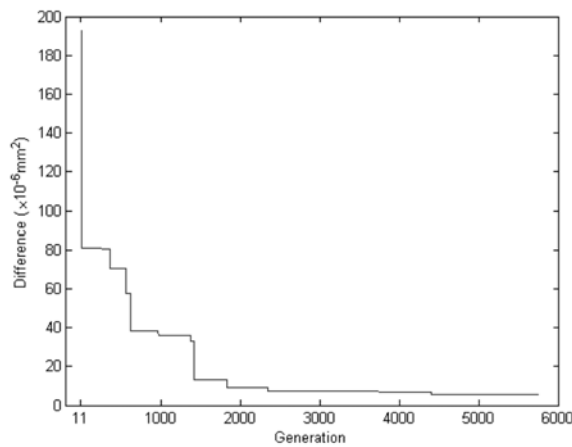


Fig. 14 Iteration information of the objective function (Approximate curve of shape)

to the desired shape. The objective function is set as the square error. The number of actuators is the constraint function and fixed to 12 for the symmetry of structure. Just like example 2, there are 40 discrete variables and 40 continuous variables in optimization model. The voltages are limited to $[-50V, 50V]$.

After 5600 iteration steps, an optimal placement can be obtained. From the optimum results, the maximum desired displacement is 0.046 mm, and the maximum actuated displacement by the reversed optimal control voltages is 0.046 mm. The square error has descended to $5.34 \times 10^{-6} \text{mm}^2$ which are closed to the result from the case 1 in which all actuators are kept. The iteration history of the objective is shown in Fig. 14. The placements of actuators for different iteration steps are shown in Figs. 15~17. The optimum control voltages are listed in Table 5.

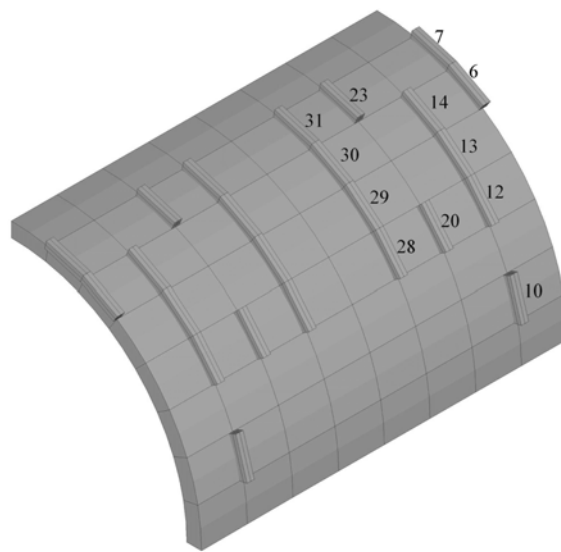


Fig. 15 Iteration result after 7 steps (Objective is descend to $716.1 \times 10^{-6} \text{mm}^2$)

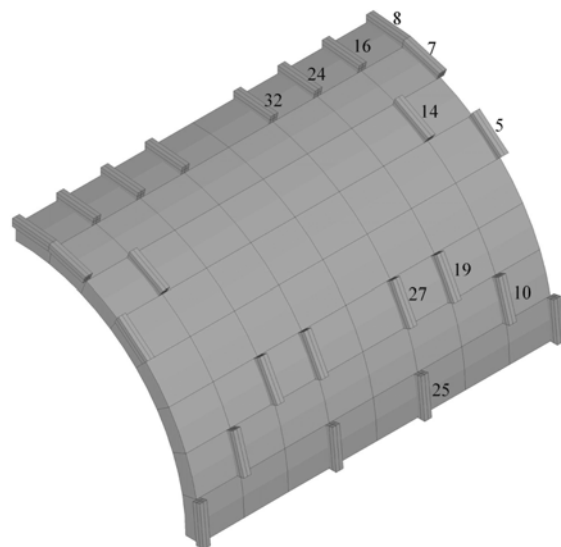


Fig. 16 Iteration result after 1600 steps (Objective is descend to $12.9 \times 10^{-6} \text{mm}^2$)

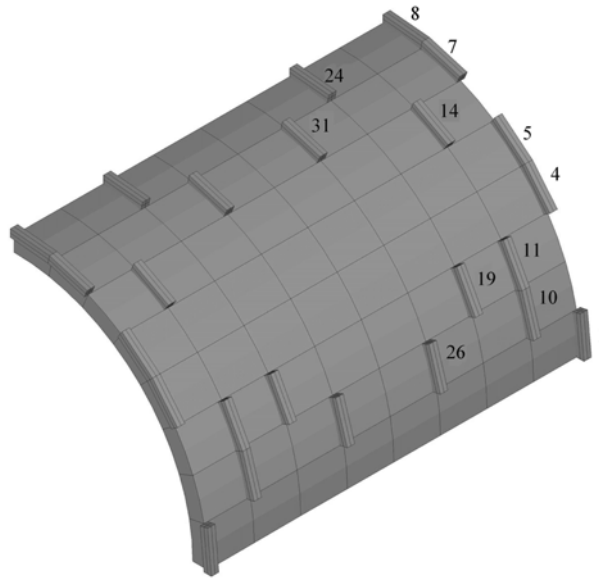


Fig. 17 Optimum distribution of piezoelectric actuators (Objective is descend to $5.34 \times 10^{-6} \text{mm}^2$)

Table 5 Voltages on distributed actuators

No.	1	4	5	7	8	10	11	14	19	24	26	31
Voltages	9.25	8.26	2.83	31.56	-2.50	-3.81	-3.60	-11.37	43.92	19.38	11.03	-6.28

6. Conclusion

A FE formulation of a new piezoelectric curve beam actuators is derived and the nodal displacement constraint equations are used to link the piezoelectric curve beam with a host shell. The accuracy of FE analysis of the piezoelectric curve beam is verified by the principle of analogy. Then LLSM is employed to get the optimum voltage distributions so that the structure shape can be effectively controlled. Furthermore, an optimal placement model of the piezoelectric curve beam actuators is proposed in the shape control system and GA with mixed binary and real codes is introduced to solve this optimization problem. Finally, the numerical examples show the shape control can reach a good precision and the optimal placement of the piezoelectric curve beam actuators can be obtained by the optimization method presented in this paper.

Acknowledgements

The project of the research presented in this paper is supported by the National Natural Science Foundation of China (10772038, 10302006 and 10421202). The authors would like to acknowledge these funding supports sincerely.

References

- Andoh, F., Washington, G., Yoon, H.S. and Utkin, V. (2004), "Efficient shape control of distributed reflectors with discrete piezoelectric actuators", *J. Intell. Mat. Syst. Str.*, **15**(1), 3-15.
- Bathe, K.J. (1996), *Finite Element Procedures*. Englewood Cliffs, NJ: Prentice Hall.
- Carbonari, R.C., Silva, E.C.N. and Nishiwaki, S. (2007), "Optimum placement of piezoelectric material in piezoactuator design", *Smart Mater. Struct.*, **16**(1), 207-220.
- Chee, C., Tong, L. and Steven, G. (2000), "A mixed model for adaptive composite plates with piezoelectric for anisotropic actuation", *Comput. Struct.*, **77**(3), 253-268.
- Chee, C.Y.K., Tong, L. and Steven, G.P. (2002), "Static shape control of composite plates using a slope-displacement-based algorithm", *AIAA J.*, **40**(8), 1611-1618.
- Cook, R.D., Malkus, D.S., Plesha, M.E. and Witt, R.J. (2007), *Concepts and Applications of Finite Element Analysis*, John Wiley & Sons.
- Degryse, E. and Mottelet, S. (2005), "Shape optimization of piezoelectric sensors or actuators for the control of plates", *ESAIM Contr. Optim. Ca.*, **11**, 673-690.
- Donthireddy, P. and Chandrashekhara, K. (1996), "Modeling and shape control of composite beams with embedded piezoelectric actuators", *Comput. Struct.*, **35**(2), 237-244.
- Fitzpatrick, B.G. (1997), "Shape matching with smart material structures using piezoceramic actuators", *J. Intell. Mat. Syst. Str.*, **8**(10), 876-882.
- Gaudenzi, P., Fantini, E., Koumoussis, V.K. and Gantes, C.J. (1998), "Genetic algorithm optimization for the active control of a beam by means of PZT actuators", *J. Intell. Mat. Syst. Str.*, **9**(4), 291.
- Ghandi, K. and Hagoood, N.W. (1996), "Nonlinear finite element modeling of phase transitions in electro-mechanically coupled material", *Proc. SPIE*, **2339**, 97-112.
- Gu, Y. and Tang, W. (2001), "A real-coded genetic algorithm for structural optimization", *2nd European Conf. on Computational Mechanics*, 370-371.
- Han, J.H. and Lee, I. (1999), "Optimal placement of piezoelectric sensors and actuators for vibration control of a composite plate using genetic algorithms", *Smart Mater. Struct.*, **8**(2), 257-267.
- Koconis, D.B., Kollar, L.P. and Springer, G.S. (1994), "Shape control of composite plates and shells with embedded actuators. 1: Voltages specified", *J. Comput. Mater.*, **28**(5), 415-458.
- Lim, K.B. (1992), "Method for optimal actuator and sensor placement for large flexible structures", *J. Guid. Control. Dynam.*, **15**(1), 49-57.
- Luo, Q. and Tong, L. (2004), "An accurate laminated element for piezoelectric smart beams including peel stress", *Comput. Mech.*, **33**(2), 108-120.
- Luo, Q. and Tong, L. (2006), "High precision shape control of plates using orthotropic piezoelectric actuators", *Finite Elem. Anal. Des.*, **42**(11), 1009-1020.
- Mukherjee, A. and Joshi, S. (2002), "Piezoelectric sensor and actuator spatial design for shape control of piezolaminated plates", *AIAA J.*, **40**(6), 1204-1210.
- Nguyen, Q., Tong, L. and Gu, Y. (2007), "Evolutionary piezoelectric actuators design optimisation for static shape control of smart plates", *Comput. Methods. Appl. M.*, **197**(1-4), 47-60.
- Onoda, J. and Hanawa, Y. (1993), "Actuator placement optimization by genetic and improved simulated annealing algorithms", *AIAA J.*, **31**(6), 1167-1169.
- Peng, F., Ng, A. and Hu, Y.R. (2005), "Actuator placement optimization and adaptive vibration control of plate smart structures", *J. Intell. Mat. Syst. Str.*, **16**(3), 263-271.
- Shah, D.K., Chan, W.S. and Joshi, S.P. (1993), "Finite element analysis of plates with piezoelectric layers", *34th AIAA/ASME/ASCE/AHS/ASC Structures, Structural Dynamics, and Materials Conf.*, 3189-3196.
- Sun, D. and Tong, L. (2005), "Design optimization of piezoelectric actuator patterns for static shape control of smart plates", *Smart Ma. Str.*, **14**(6), 1353-1362.
- Tang, W., Tong, L. and Gu, Y. (2005), "Improved genetic algorithm for design optimization of truss structures with sizing, shape and topology variables", *Int. J. Numer. Meth. Eng.*, **62**(13), 1737-1762.
- Tang, W.Y. and Gu, Y.X. (2002), "Improvements on genetic algorithm for truss structural optimization", *Journal of Mechanical Strength (in Chinese)*, **24**(1), 10-12.
- Tiersten, H. F. (1969), *Linear piezoelectric plate vibrations*, Plenum.

- Tzou, H.S. and Tseng, C.I. (1990), "Distributed piezoelectric sensor/actuator design for dynamic measurement/control of distributed parameter systems: A piezoelectric finite element approach", *J. Sound Vib.*, **138**(1), 17-34.
- Xie, Y.M. and Steven, G.P. (1997), *Evolutionary Structural Optimization*, Springer New York.

CC